CANCER GENOMICS & PROTEOMICS *19*: 540-555 (2022)
doi:10.21873/cgp.20339

Disruption of Lipid Raft Microdomains, Regulation of CD38, TP53, and MYC Signaling, and Induction of Apoptosis by Lomitapide in Multiple Myeloma Cells

MOHAMED E. M. SAEED[1], JOELLE C. BOULOS[1], SABRINA B. MÜCKLICH[1], ELLEN LEICH[2,3], MANIK CHATTERJEE[3], SABINE M. KLAUCK[4] and THOMAS EFFERTH[1]

[1]*Department of Pharmaceutical Biology, Institute of Pharmaceutical and Biomedical Sciences, Johannes Gutenberg University, Mainz, Germany;*
[2]*Julius Maximilian University, Institute of Pathology, Würzburg, Germany;*
[3]*Comprehensive Cancer Center Mainfranken, Translational Oncology, University Hospital of Würzburg, Würzburg, Germany;*
[4]*Division of Cancer Genome Research, German Cancer Research Center (DKFZ), German Cancer Consortium (DKTK), National Center for Tumor Diseases (NCT), Heidelberg, Germany*

Abstract. *Background/Aim: Multiple myeloma (MM) is characterized by accumulation of a malignant clone of plasma cells in the bone marrow. Curative treatments are not yet available. Therefore, we undertook a drug repurposing approach to identify possible candidates from a chemical library of 1,230 FDA-approved drugs by virtual drug screening. As a target, we have chosen the non-receptor Bruton's tyrosine kinase (BTK) which is one of the main regulators of the MM biomarker CD38. Materials and Methods: In silico virtual screening was performed by using PyRx. Flow cytometry was applied for cell cycle and apoptosis analysis. Furthermore, protein and gene expression was determined by western blotting and microarray hybridization. Lipid raft staining was observed by confocal microscopy. Results: The in silico identified lipid-lowering lomitapide presented with the strongest cytotoxicity among the top 10 drug candidates. This drug arrested the cell cycle in the G_2/M phase and induced apoptosis in MM cells. Western blot analyses revealed that treatment with lomitapide induced cleavage of the apoptosis regulator PARP and reduced the expression of CD38, an integral part of lipid rafts. Using confocal microscopy, we further observed that lipid raft microdomain formation in MM cells was inhibited by lomitapide. In four MM cell lines (KMS-12-BM, NCI-H929, RPMI-8226, and MOLP-8) treated with lomitapide, microarray analyses showed not only that the expression of CD38 and BTK was down-regulated, but also that the tumor suppressor gene TP53 and the oncogene c-MYC were among the top deregulated genes. Further analysis of these data by Ingenuity pathway analysis (IPA) suggested that lomitapide interferes with the cross-talk of CD38 and BTK and apoptosis-regulating genes via TP53 and c-MYC. Conclusion: Lomitapide treatment led to disruption of lipid raft domains and induction of pro-apoptotic factors and might, therefore, be considered as a potential therapeutic agent in MM.*

Correspondence to: Thomas Efferth, Johannes Gutenberg University, Institute of Pharmaceutical and Biomedical Sciences, Staudinger Weg 5, 55128 Mainz, Germany. Tel: +49 61313925751, e-mail: efferth@uni-mainz.de

Key Words: Cholesterol, drug repurposing, lipid rafts, microarray analyses.

Multiple myeloma (MM) is characterized by the expansion of a malignant plasma cell clone in the bone marrow (BM) leading to elevated levels of monoclonal proteins in the serum and/or urine and associated organ dysfunctions, *e.g.*, hematopoietic insufficiency, osteolytic bone disease, and kidney damage (1). At an advanced disease stage, MM cells can become independent of the BM microenvironment and grow in the peripheral blood and other extramedullary sites such as soft tissue and organs (2, 3). The malignant transformation originated from post-germinal center B cells *via* a multistep process involving the acquisition of genetic alterations and BM microenvironmental changes (4, 5). MM is the second most frequent blood cancer with an annual age-adjusted incidence of six cases per 100,000 persons in the

USA and Europe (6). The global incidence is higher in developed countries, such as the United States, Western Europe, and Australia, which is attributed to the availability of better diagnostic techniques, as well as a greater clinical awareness of the disease (7). The incidence is higher in black people and lower in Asians than in white people (8). Although substantial therapeutic progress has been achieved in the past two decades, curative treatments are not yet available.

Lipid rafts are membrane microdomains enriched in saturated phospholipids, sphingolipids, cholesterol, and a variety of signaling and transport proteins (9). Lipid rafts play a vital role in triggering apoptosis, signal-transduction, immune response, and in many pathological situations cardiovascular and neurological diseases (9, 10). CD38 is a transmembrane glycoprotein associated with lipid rafts that is highly and uniformly expressed on MM cells but only at relatively low levels on normal lymphoid and myeloid cells (11, 12). CD38 is an adhesion molecule and ectoenzyme involved in the catabolism of nicotinamide adenine dinucleotide (NAD^+) and nicotinamide adenine dinucleotide phosphate (NADP) (13). It is also considered as a receptor if ligated to CD31 or agonistic antibodies, triggering complex transmembrane signaling. This ligation potentially leads to activation of B and T lymphocytes and dendritic cells, the proliferation of T lymphocytes, and the production of pro-inflammatory and regulatory cytokines by monocytes and natural killers (14-18). The rearrangement of the cell surface with the formation of glycosphingolipid- and cholesterol-rich plasma membrane precedes the endocytosis of human CD38 molecule suggesting these raft microdomains mediate CD38 translocation at the intracellular level (19). Of note, the downstream signaling transduction of CD38 is regulated by activation of the non-receptor Bruton's tyrosine kinase (BTK). The BTK is encoded by the X-linked immunodeficiency (*xid*) gene, and the B lymphocytes of immunodeficient xid mice reveal a missense mutation at a normally conserved residue in the unique region of BTK (20). There is a cross-talk between CD38 and BTK. B lymphocytes from unstimulated xid mice are unresponsive to CD38 stimulation both in terms of proliferative response and surface antigen modulation. Therefore, BTK is either an integral component or an indirect regulator of the CD38-induced signal transduction pathway (21). Furthermore, BTK is highly expressed in MM cells (22) and plays a role in signal transduction pathways for mature B-lymphocytes and plasma cells (23). Poor prognosis is a common trait of MM patients with elevated levels of BTK (22).

Lomitapide is a lipid-lowering drug prescribed for the treatment of homozygous familial hypercholesterolemia (HoFH), a disease that is characterized by severe hypercholesterolemia and very premature atherosclerotic cardiovascular disease (ASCVD) (24). Lomitapide inhibits the microsomal triglyceride transfer protein (MTTP), an enzyme responsible for assembly of very low-density lipoprotein (VLDL) and chylomicron *via* loading of triglyceride onto apolipoprotein B. Inhibition of MTTP results in a reduction of VLDL release and VLDL-mediated triglyceride secretion that leads to a reduction of LDL-cholesterol (LDL-C) and total cholesterol (TC) levels in plasma.

Drug repositioning is a process of finding novel uses of a specific drug outside its original medical indication. This concept is also known as drug redirecting, repurposing, rediscovery, or reprofiling (25). The drug repositioning approach surpasses the *de novo* drug discovery in regard to perceived safety and tolerability knowledge of the existing approved drugs. In the past, various approved drugs have been redirected for cancer treatment. Thalidomide was reapproved for MM in 2006. It was initially introduced as oral sedative and anti-emetic drug to treat morning sickness from the 1950s to the early 1960s. Due to its teratogenicity (congenital defects), it was withdrawn from the market in 1962 (26). Moreover, there is a long history in repurposing the anti-malarial artemisinin and its derivatives for cancer treatment from our own group (27, 28), and several clinical phase I/II trials with human as well as veterinary tumors have been accomplished (29-31).

In this study, we systematically implemented a drug repositioning approach to redirect a previously approved drug for the treatment of MM. As a starting point, we determined the CD38 regulator BTK as molecular target that is highly expressed in MM cells. Afterwards, we performed *in silico* virtual screening using a chemical library of 1230 FDA-approved drugs. Lomitapide was among the top compounds with high binding affinity towards BTK. Furthermore, the preliminary *in vitro* cytotoxicity testing showed that lomitapide was the most active compound towards MM cell lines. We further investigated the cytotoxic activity and mechanism of action of lomitapide in 9 MM cell lines. We identified lipid raft microdomains as target for lomitapide by which cell cycle arrest and apoptosis was triggered in MM cells. The lipid raft constituent CD38 was down-regulated by lomitapide. By microarray analyses, TP53 and c-MYC were identified as CD38 regulators.

Materials and Methods

Virtual drug screening in silico. *In silico* virtual screening by PyRx is a predictive computational drug discovery tool to screen libraries of compounds against potential target macromolecules. X-ray crystallography-based structures of BTK (PDB ID: 4RX5) was obtained from Protein Data Bank (32). The FDA-approved drug library was downloaded from the ZINC database (33) as one spatial data file format. The energy of these approved drugs was minimized and converted to docking pdbqt format using open babel in PyRx tool. A total of 1230 FDA-approved drugs were docked on BTK after centering the binding geometry (grid box) to cover the whole protein.

Table I. *Characteristics of human multiple myeloma cell lines*.

Cell line	Origin	Cell type	Culture type
AMO-1	Established from the ascetic fluid of a 64-year-old woman with plasmacytoma in 1984	Plasmacytoma	Suspension cells
JJN-3	Established from bone marrow of a 57-year-old woman with plasma cell leukemia at diagnosis in 1987	Plasma cell leukemia	Suspension cells
KMS-11	Established from pleural effusion of a 67-year-old woman	Multiple myeloma	Suspension and adherent cells
KMS-12-BM	Established from bone marrow of a 64-year-old woman with multiple myeloma in 1988	Multiple myeloma	Suspension cells
L-363	Established from the peripheral blood of a 36-year-old woman with plasma cell leukemia in 1977	Plasma cell leukemia	Suspension cells
MOLP-8	Established from the peripheral blood of a 52-year-old Japanese man with multiple myeloma in 2002	Multiple myeloma	Suspension cells
NCI-H929	Established from pleural effusion of a 62-year-old white woman with myeloma at relapse	Multiple myeloma	Suspension cells
OPM-2	Established from the peripheral blood of a 56-year-old-woman with multiple myeloma in leukemic phase in 1982	Multiple myeloma	Suspension cells
RPMI-8226	Established from the peripheral blood of a 61-year-old man with multiple myeloma	Multiple myeloma	Suspension and adherent cells

The scoring function [binding energy (kcal/mol)] was calculated using the standard protocol of Lamarckian genetic algorithm (34).

Cell lines. The 9 MM cell lines listed in Table I are originated from the Leibniz Institute DSMZ-German Collection of Microorganisms and Cell Cultures (Braunschweig, Germany). The cells were propagated in RPMI 1640 medium supplemented with 10% FBS and 1% penicillin/streptomycin (Invitrogen/Thermo Fisher Scientific, Darmstadt, Germany) and incubated in humidified 5% CO_2 atmosphere at 37˚C.

Cell viability assay. The cell viability of selected FDA approved drugs was determined by resazurin assay. The resazurin dye was used to evaluate the biocompatibility of medical materials by measuring innate metabolic activity using a redox indicator. Viable cells with active metabolism can reduce resazurin to strongly-fluorescent dye resorufin (35). The protocol we are suing has been published (36, 37). The IC_{50} values have been calculated from dose response. Each assay was executed three times independently with six replicates each. All IC_{50} values are expressed as mean±standard deviation (SD).

Cell cycle analysis by flow cytometry. Flow cytometric analysis was performed to detect apoptotic cells with fractional DNA content. In this method, cellular DNA content is being determined by staining the cells with propidium iodide (PI) that functions as the DNA fluorochrome. PI binds DNA by intercalating between base pairs. It can be excited at 488 nm, and the cells can be distributed in four major phases of the cell cycle (sub-G_1, G_0/G_1, S, G_2/M). Quantitation of apoptotic cells was determined as the percentage of cells in the sub-G_1 region (hypodiploidy) in cell cycle analysis.

MM cell line NCI-H929 (10^6 cells/well) was treated with varying concentration of lomitapide (Sigma-Aldrich, Taufkirchen, Germany) (0.5×IC_{50}, IC_{50}, and 2×IC_{50}) for 24 h, 48 h and 72 h at 37˚C. Then, the cells were harvested and washed two times with cold PBS (Thermo Fisher Scientific, Darmstadt, Germany). The cells were fixed using 80% cold ethanol and incubated for 3 h at –20˚C. After washing the cells with PBS, 10 μg/ml RNase A (AppliChem LifeScience, Darmstadt, Germany) were added for 10 min for optimal DNA resolution. Afterwards, 50 μg/ml PI (Sigma-Aldrich) were added to the cells and the fluorescence was measured after 15 min with the Accuri™ C6 cytometer (BD Biosciences, Heidelberg, Germany) with 488 nm excitation. For each treatment period (24 h, 48 h and 72 h), the experiments were performed in triplicates. The results were analyzed using Excel (Microsoft Corp., Redmond, WA, USA) and FlowJo (Celeza, Olten, Switzerland).

Apoptosis assay by annexin V/PI staining. Annexin V is a calcium-dependent phospholipid that binds to phosphatidylserine (PS) that translocates from the intracellular compartment of the plasma membrane to the external leaflet upon initiation of apoptosis. Propidium iodide (PI) is excluded by living or early apoptotic cells with intact membranes and stains late apoptotic or necrotic cells with red fluorescence due to DNA intercalation. Therefore, cells with annexin V (–) and PI (–) are considered to be alive while cells with annexin V (+) and PI (–) are in early apoptosis. Necrotic cells or cells in late apoptosis are both annexin V and PI positive.

The MM cell line NCI-H929 (10^6 cells/well) was treated with varying concentrations of lomitapide (IC_{50}, 2×IC_{50}, and 4×IC_{50}) for 72 h. Afterwards, cells were collected and washed with PBS (Thermo Fisher Scientific). Cells were stained with annexin V and PI binding buffer (Invitrogen/Thermo Fisher Scientific) according to the manufacturer's protocol. Subsequently, 3×10^4 cells were gated and measured with the Accuri™ C6 cytometer (BD Biosciences). The annexin V-FITC signal was measured with 488 nm excitation and detected using a 530/30 nm band pass filter. The PI signal was analyzed with 561 nm excitation and detected using a 610/20 nm band pass filter. All parameters were plotted on a logarithmic scale. Cytographs were analyzed using the BD Accuri C6 software (BD Biosciences).

Analysis of protein expression via western blotting. Whole protein fractions were extracted from the KMS-12-BM cells using M-

PER™ mammalian protein extraction buffer (Thermo Fisher Scientific) containing protease and phosphatase inhibitors. Afterwards, sodium dodecyl sulfate (SDS) polyacrylamide gel electrophoresis was carried out to separate the proteins and the lysates were then transferred to polyvinylidene fluoride membranes (Ruti®-PVDF) (Merck Millipore, Schwalbach, Germany) for western blotting. Five percent of bovine serum albumin was used to block the membranes and then the membranes were incubated with specific primary antibodies against CD38 (1:1,000) (Cell Signaling Technology Europe B.V., Frankfurt, Germany), PARP (1:1,000) (Cell Signaling Technology Europe), and β-actin (1:2,000) (Cell Signaling Technology Europe). The blots were probed with horseradish 2 h at room temperature. Finally, Luminata™ Classico Western HRP substrate (Merck Millipore) was added for 5 min in the dark. Alpha Innotech FluorChem Q system (Biozym, Oldendorf, Germany) was used for documentation and band analysis.

Transcriptomic profiling and signaling pathway analysis. Four MM cell lines (MOLP-8, RPMI-8226, NCI-H929, and KMS-12-BM) were treated with IC_{50} concentration of lomitapide. After 24 h, the total mRNA was extracted using InviTrap® spin universal RNA kit (STRATEC Molecular GmbH, Berlin, Germany) according to the manufacturer's protocol. The quality of total RNA was validated by gel analysis on an Agilent 2100 Bioanalyzer (Agilent Technologies GmbH, Berlin, Germany). Only samples with RNA index values greater than 6.60 were selected for expression profiling. Microarray experiments were conducted in duplicates for treated and untreated samples by the Genomics and Proteomics Core Facility at the German Cancer Research Center (DKFZ, Heidelberg) using Illumina Human Sentrix12 Bead Chip arrays (Illumina Inc., San Diego, CA, USA). Biotin-labeled cRNA samples for hybridization Bead Chip arrays were prepared according to Illumina's recommended sample labeling procedure based on the modified Eberwine protocol (38). Microarray scanning was done using a Beadstation array scanner, setting adjusted to a scaling factor of 1 and PMT settings at 430. Data was extracted for each bead individually, and outliers were removed if the MAD (median absolute deviation) was greater than 2.5. Data analysis was performed by using the quantile normalization algorithm without background subtraction, and differentially regulated genes were defined by calculating the standard deviation differences of a given probe in a one-by-one comparison of samples or groups. Chipster® data analysis platform (http://chipster.csc.fi/) was used for statistical analysis of the expression data. These steps include filtering of genes by standard deviation of deregulated genes and a subsequent calculation of significance using two group *t*-test ($p<0.05$). The statistically significant deregulated gene dataset was subjected to Ingenuity Pathway Analysis (IPA, Ingenuity Systems, Redwood City, CA, USA) to explore possible signaling pathways, the upstream regulators, and the molecular networks. Firstly, the data were analyzed by the core analysis tool of IPA to determine cellular networks and functions that might be affected by lomitapide treatment. Following this approach, the core analyses results were subjected to the "comparison analysis" tool of IPA, allowing the possibility to find possible common upstream regulators that might be responsible for lomitapide's activity in all treated MM cell lines.

Lipid raft staining and confocal microscopy. NCI-H929 cells (1×10^6 cells/well) were treated with varying concentrations of lomitapide ($0.25\times IC_{50}$, $0.5\times IC_{50}$, IC_{50} and $2\times IC_{50}$) for 24 h. The cells were stained following the manufacturer's protocol using Vybrant® lipid raft labeling kit (Thermo Fisher Scientific) Briefly, the living cells were labeled with cholera toxin subunit B (CT-B) conjugated with Alexa flour 594 (1 μg/ml) for 10 min at 4˚C. Afterwards, CT-B–labeled lipid rafts on the cells were cross-linked with anti–CT-B antibody (1:200) for 15 min at 4˚C. Next, the cells were washed three times with PBS and finally mounted on a μ-Slide VI0.4 microscopy chamber (ibidi GmbH, Martinsried, Germany). Fluorescence and differential interference contrast (DIC) microscopic images were acquired with a Spinning Disc Confocal Microscope (VisiScope 5-Elements, Visitron Systems GmbH, Puchheim, Germany) based on a Nikon Ti2-E and a CSU-W1 (Yokogawa) located at the Microscopy and Histology Core Facility of the Institute of Molecular Biology (Mainz, Germany). Following imaging settings were used: 405 nm and 594 nm laser excitation, filters (ET460/50m and 565/133 Bright Line HC), 60× water immersion objective (NA 1.2, CFI Plan Apo VC), sCMOS camera (BSI, Photometrics, Scientifica Ltd., Uckfield, East Sussex, UK), VisiView Software 4.5 (Visitron Systems).

Table II. *Binding energies of the top 10 FDA-approved drugs to BTK as identified by virtual drug screening using PyRx.*

Compound	Binding energy (kcal/mol)	Indication
Saquinavir	–15.1	HIV-1 infection
Lopinavir	–13.1	HIV-1 infection
Ledipasvir	–12.9	Chronic hepatitis C virus infection
Gadofosveset	–12.7	Contrast agent in magnetic resonance angiography
Lomitapide	–12.7	Lipid-lowering drug against familial hypercholesterolemia
Loperamide	–12.5	Acute diarrhea, irritable bowel syndrome
Butrans	–12.5	Severe pain killer
Ergotamine	–12.3	Migraine-related headache
Conivaptan	–12.3	Euvolemic hyponatremia
Darifenacin	–12.0	Urinary incontinence

Results

In silico virtual screening of FDA approved drugs. In order to have insight about possible candidates that target BTK, we performed *in silico* virtual screening of 1,230 FDA approved drugs using PyRx. As shown in Table II, the binding energies of the top 10 compounds varied from –15.1 kcal/mol to –12 kcal/mol. The top three drugs were antiviral agents whereas the rest were prescribed for various indications such as hypercholesterolemia, euvolemic hyponatremia, antidiarrheal, and antiemetic agents.

In vitro cell viability screening revealed lomitapide as most active drug. To corroborate the reliability of the *in silico* virtual screening results, we selected six compounds (saquinavir, lopinavir, ledipasvir, conivaptan, lomitapide, and

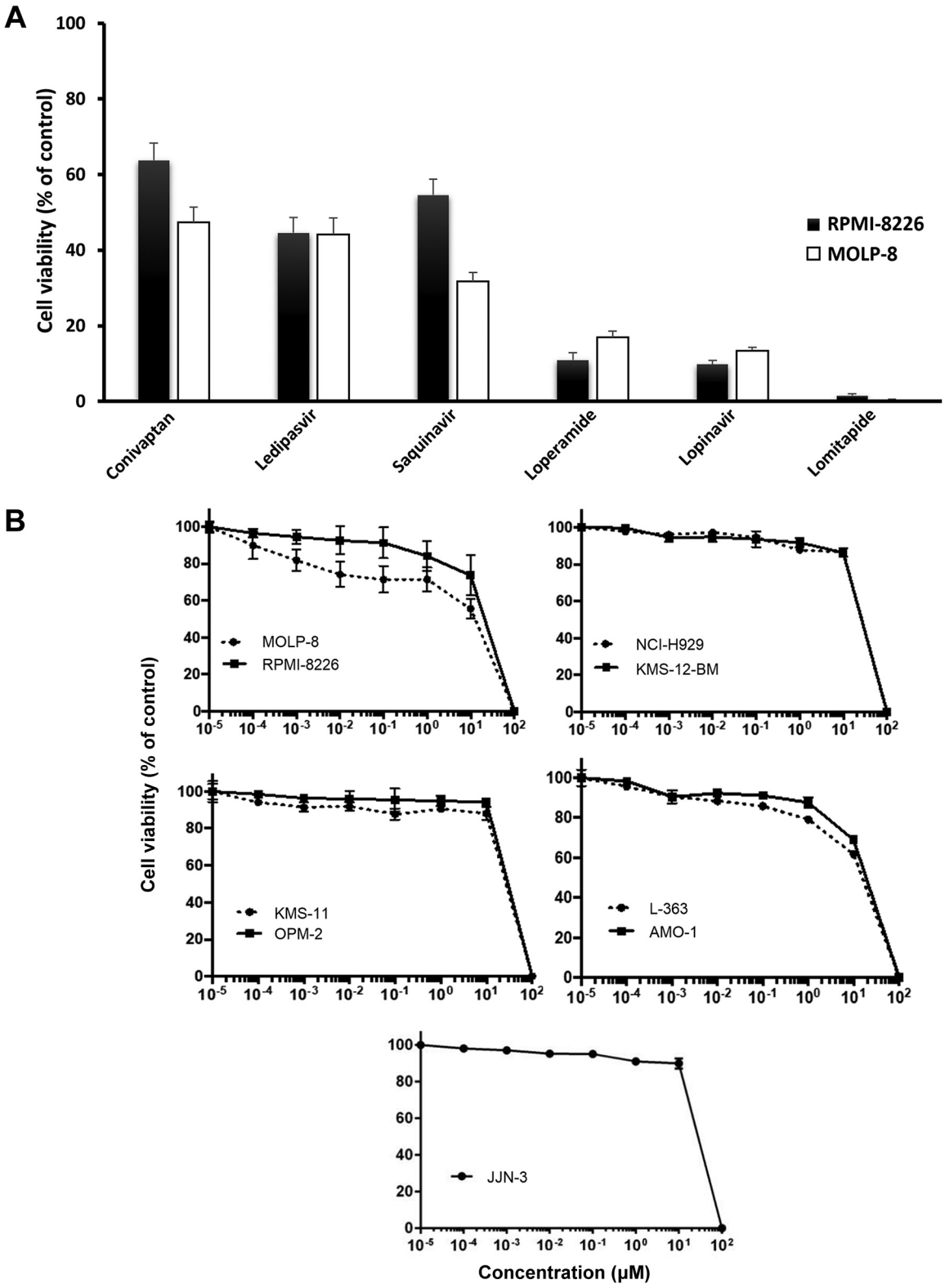

Figure 1. *(A) Preliminary screening of selected FDA-approved drugs in MOLP-8 and RPMI-8226 multiple myeloma (MM) cell lines as determined by resazurin assay. (B) Dose response curves of 9 MM cell lines (MOLP-8, RPMI-8226, NCI-H929, KMS12-BM, KMS-11, OPM-2, L363, AMO-1 and JJN-3) for lomitapide as determined by the resazurin assay. Each assay was performed three times and each point in the curve represents the mean±standard deviation (SD).*

Table III. *IC_{50} values of multiple myeloma cell lines for lomitapide as determined by resazurin-based cytotoxicity assay.*

Cell line	IC_{50} (μM)
MOLP-8	8.17±3.10
RPMI-8226	17.14±3.80
NCI-H929	26.87±5.90
KMS-12-BM	24.11±5.30
KMS-11	24.90±6.47
OPM-2	28.52±7.29
AMO-1	20.85±0.43
L-363	18.84±5.27
JJN-3	25.89±5.96

loperamide) from the top 10 virtual screening list for *in vitro* cytotoxicity screening on two exemplarily selected MM cell lines (MOLP-8 and RPMI-8226). The drugs were screened at a fixed concentration (10 μM). The results revealed that only three compounds (lopinavir, lomitapide, and loperamide) have the ability to kill more than 80% of the two MM cells lines (Figure 1A). Interestingly, lomitapide was the most active drug on both MM cell lines. Therefore, it was considered for further analysis.

Cell viability dose response curves of lomitapide-treated MM cell lines. We used the resazurin cytotoxicity assay to investigate the cytotoxic potential of lomitapide towards MM cells. Nine MM cell lines were treated with varying concentrations of lomitapide range from 10^{-5} to 10^{2} μM. As shown in Figure 1B and Table III, the dose response curves were plotted and IC_{50} values were calculated.

Lomitapide induced apoptosis in MM cells. Following our efforts to elucidate the mechanism of action of lomitapide, we exemplarily assessed cell-cycle progression in NCI-H929 cells. The cells were treated with varying concentrations of lomitapide ($0.5\times IC_{50}$, IC_{50}, and $2\times IC_{50}$) for 24 h, 48 h and 72 h at 37˚C. As shown in Figure 2A-C, the treated cells showed a typical DNA histogram that represented sub-G_0/G_1, G_0/G_1, S, and G_2/M phases of cell cycle. The percentage of sub-G0/G1 significantly increased after cells were treated with lomitapide compared to the DMSO-treated control cells. The results revealed a dose- and time-dependent elevation of sub-G_0/G_1 population in the cells upon lomitapide treatment, suggesting that lomitapide triggered cellular apoptosis in MM cells.

Furthermore, to verify the apoptosis-triggering effect in a second cell line, we assessed PARP cleavage in KMS-12-BM cells treated with lomitapide (IC_{50}, and $2\times IC_{50}$) for 24 h. Indeed, PARP was clearly cleaved in treated cells (Figure 2D). To further confirm the induction of apoptosis, we performed annexin V/PI staining. As shown in Figure 3, more than 80% of the cells appeared in late apoptosis upon treating NCI-H929 cells with lomitapide (annexin V+/PI+).

Lomatipide significantly down-regulated the expression of CD38. Since CD38 is considered as important player in MM, we evaluated its expression by western blotting. Five cell lines (MOLP-8, RPMI-8226, NCI-H929, KMS-12-BM, and L363) expressed CD38 while AMO-1, JJN-3, KMS-11, and OPM-2 cells did not. We selected KMS-12-BM cells and treated them with different concentrations of lomitapide ($0.5\times IC_{50}$, IC_{50}, and $2\times IC_{50}$) for 24 h at 37˚C. The expression of CD38 was down-regulated in a dose-dependent manner (Figure 2E).

Lomitapide disrupted lipid raft formation. Based on two facts (1) lomitapide lowers cholesterol levels which is highly enriched in lipid rafts microdomains and (2) the disruption of lipid rafts triggers apoptosis *via* recruiting and clustering of the death receptors (39, 40), we hypothesized that lomitapide may induces apoptosis in MM cells *via* cholesterol depletion and subsequently rafts disruption. Therefore, we investigated the lipid rafts arrangements upon addition of lomitapide in varying concentrations to NCI-H929 cells. Remarkably, lomitapide disrupted the lipid rafts arrangements in a dose-dependent manner (Figure 4).

Gene expression profiling of lomitapide-treated MM cell lines highlighting TP53 and MYC as common molecular key players. Gene expression analyses were carried out to get a deeper insight into the molecular modes of action of lomitapide in MM cells. A total number of 884 genes were commonly deregulated in four CD38-positive MM cell lines investigated (MOLP-8, RPMI-8226, NCI-H929, and KMS-12-BM). The deregulated genes were involved in various cellular pathways such as DNA damage, cellular death, cell cycle, lipid metabolism, oxidative phosphorylation, and mitochondrial dysfunction.

A striking result emerging from the microarray data was that both *TP53* and *c-MYC* were suggested by the "upstream regulator analysis" function of the IPA program as the top common upstream regulators of the four lomitapide-treated MM cell lines (Figure 5). Therefore, we searched which genes deregulated by lomitapide underlie TP53 regulation (Figure 6). The top up-regulated genes of activated *TP53* were *CCL3L3, ATF3, JUN, KLF6, ASS1, CCL5, CAV1, NFKB2, NFKBIA, PIM1, ATF4, DUSP1*, *TNFRSF10B,* and *ICAM1* whereas the top down-regulated genes were *ID3, FABP5, ITGB7, MRPL12, ATPMC1, ADA, COQ3, NME1, MGST2, MRTO4, EIF4A1,* and *ALDOA*. By using IPA, we did the same for *c-MYC* to identify the c-MYC-regulated genes upon lomitapide treatment (Figure 7). The top down-regulated genes of inhibited *c-MYC* were *SLC3A2, JUN, KLF6, ASS1, CAV1, BCAT1, SHMT2, NFKBIA, SAT1, OAS1, ATF4, TNFRSF10B, FBXO32,* and *ICAM1* whereas the top

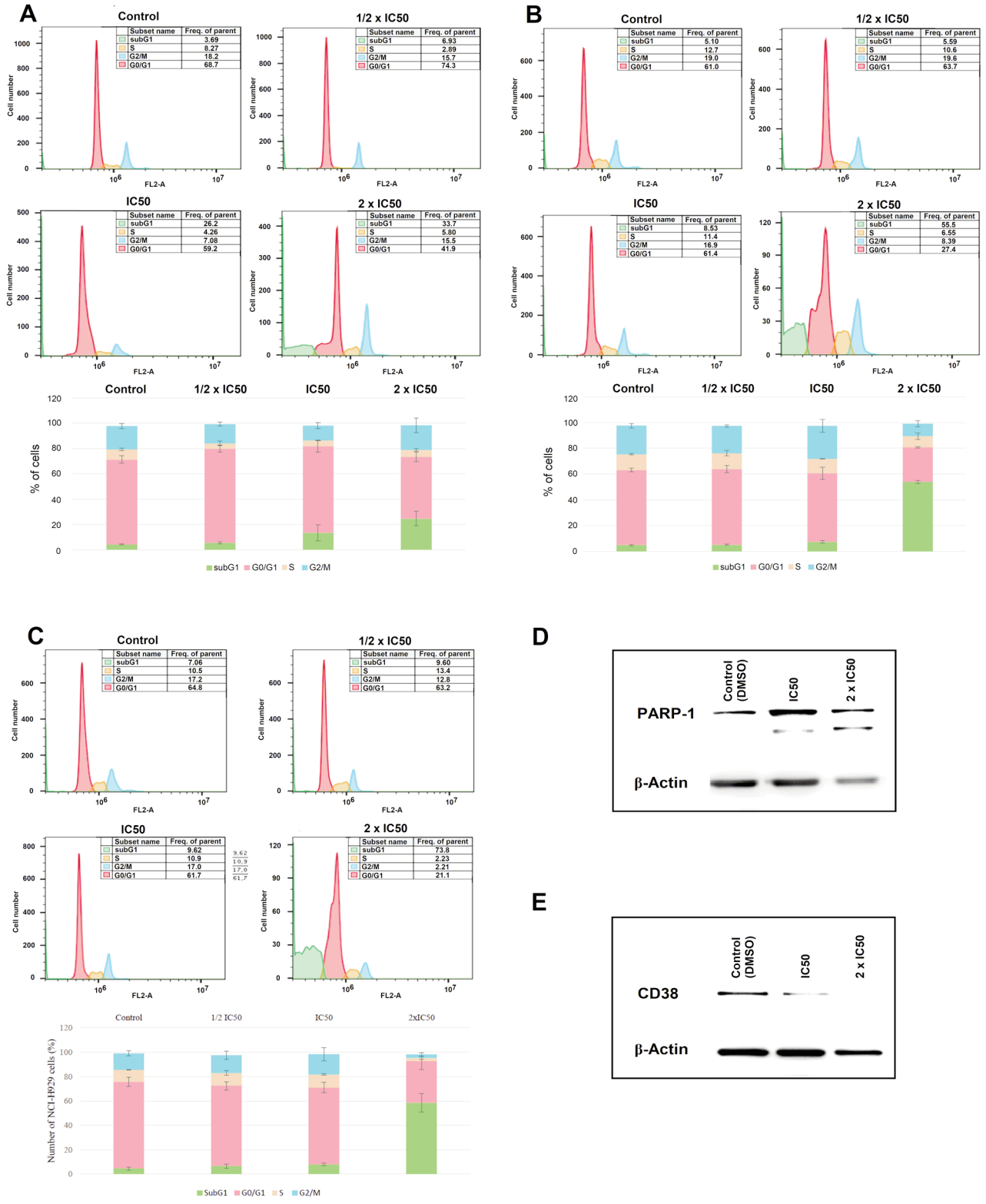

Figure 2. *Cell cycle distribution of NCI-H929 cells treated with varying concentrations of lomitapide (0.5×IC_{50}, IC_{50}, and 2×IC_{50}) for (A) 24 h, (B) 48 h, and (C) 72 h incubation at 37°C. Data points are means of at least three independent experiments with standard error of the mean (SEM). Western blot analyses of KMS-12BM cells treated with varying concentrations of lomitapide (IC_{50}, and 2×IC_{50}) to detect (D) PARP-1 cleavage and (E) CD38 expression.*

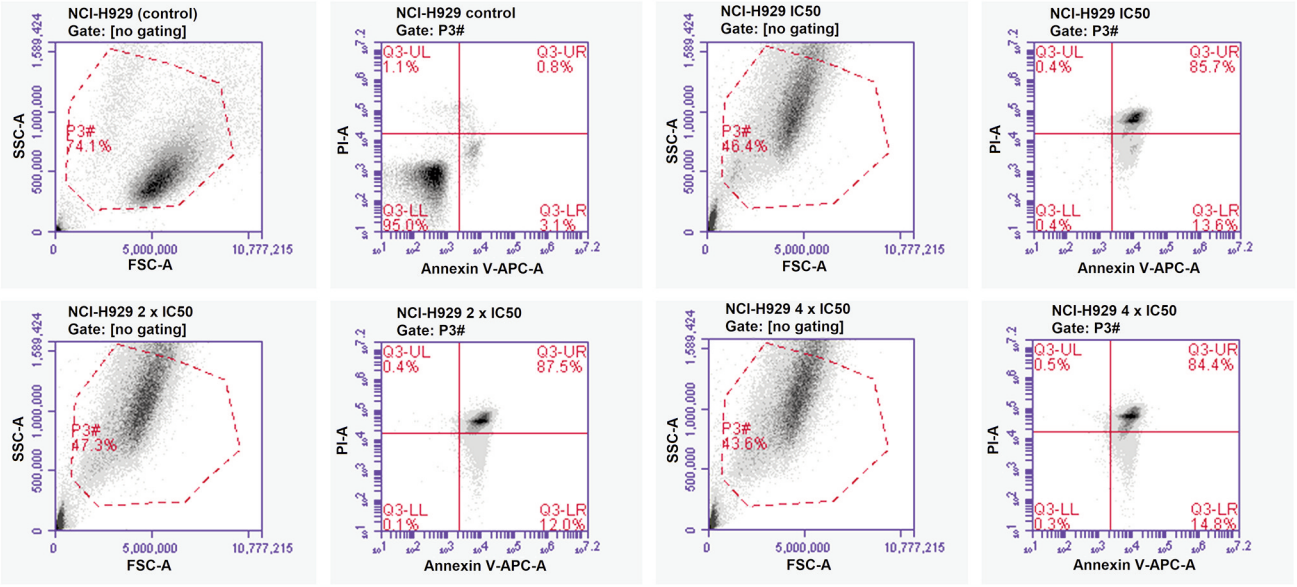

Figure 3. *Apoptosis assay via annexin V/PI staining in NCI-H929 cells treated with varying concentrations of lomitapide (IC_{50}, $2\times IC_{50}$, and $4\times IC_{50}$).*

down-regulated genes of inhibited *c-MYC* were *ID3, FABP5, GAMT, RPS7, TNFRSF8, MRPL12, PGAM1, BZW2, RPL6, RANBP1, NME1, HNRNPA1, EIF4A1, PSMB8, RUVBL1, SRM, NOP56, PHB, HNRNPD, HSPD, PFKM, ALDOA,* and *LDHA*. Interestingly, CD38 and its regulator BTK were both found to be down-regulated following lomitapide treatment. Using the IPA "pathway builder" tool, a schematic pathway elucidating the cross-talk between CD38, BTK, and apoptosis regulators genes is shown in Figure 8.

Discussion

The development of bioinformatics and biological computation tools have spurred researchers to dig into basic genomic, proteomic, and other "omics" data and exploit these data for the identification of drug targets and development of drugs for new disease indications. Recently, drug repositioning for cancer treatment emerged as a dynamic field of drug development due to the fast growth of bioinformatic knowledge and the availability of oncogenomic data. This concept could considerably lessen the risks of development and the costs, and shorten the lag between drug discovery and availability (41). In this study, our drug repositioning strategy was initially based on *in silico* virtual screening of FDA-approved drugs against a known CD38's regulator BTK that plays a role as signal transducer in MM. The virtual screening outcomes were followed by *in vitro* cytotoxicity screening and finally elucidation of the mechanism of action of the selected compound towards MM cells. The hit rate of our *in silico* approach was plausible, since 50% of our selected drugs for *in vitro* screening were indeed found to be active against MM cells. Compared to literature data, this hit rate is remarkably high (42). Lomitapide achieved more than 95% killing activity towards RPMI-8226 and MOLP-8 cells at a fixed concentration (10 μM). This result impelled us to further illustrate the mode of action of lomitapide on MM cells.

Lomitapide is a lipid lowering agent notably reducing the cholesterol level by preventing the very low-density lipoprotein (VLDL) assembly. Since cholesterol and triglycerides are risk factors for the development of tumors (43), it is reasonable to propose that lomitapide may be repurposed for cancer prevention and treatment. Cholesterol is an integral part of the plasma membrane of mammalian cells that is assembled in the lipid rafts to maintain structural integrity and modulate fluidity of the cells. Additionally, the membrane lipid rafts recruit a large number of cancer-related signaling and adhesion molecules that have a role in membrane trafficking and downstream signal transduction (44). Moreover, cholesterol has been linked to survival and enhancing the proliferation of MM cells (45) and overexpression of LDL receptor in MM cells indicated that LDL-cholesterol is a vital player for their growth (46). Another class of lipid lowering drugs, the statins, exert their antineoplastic effects through triggering apoptosis or mediating growth suppressions of malignant cells (47, 48). The conspicuous observations emerging from cell cycle analysis and lipid raft disruption in the current study indicated that lomitapide triggered apoptosis in MM cells. This concurs well with previous findings reporting that the depletion of membrane cholesterol leads to the disruption of membrane lipid rafts, blockage of the adhesion and migration processes of cancer cells, and induction of apoptosis (49, 50).

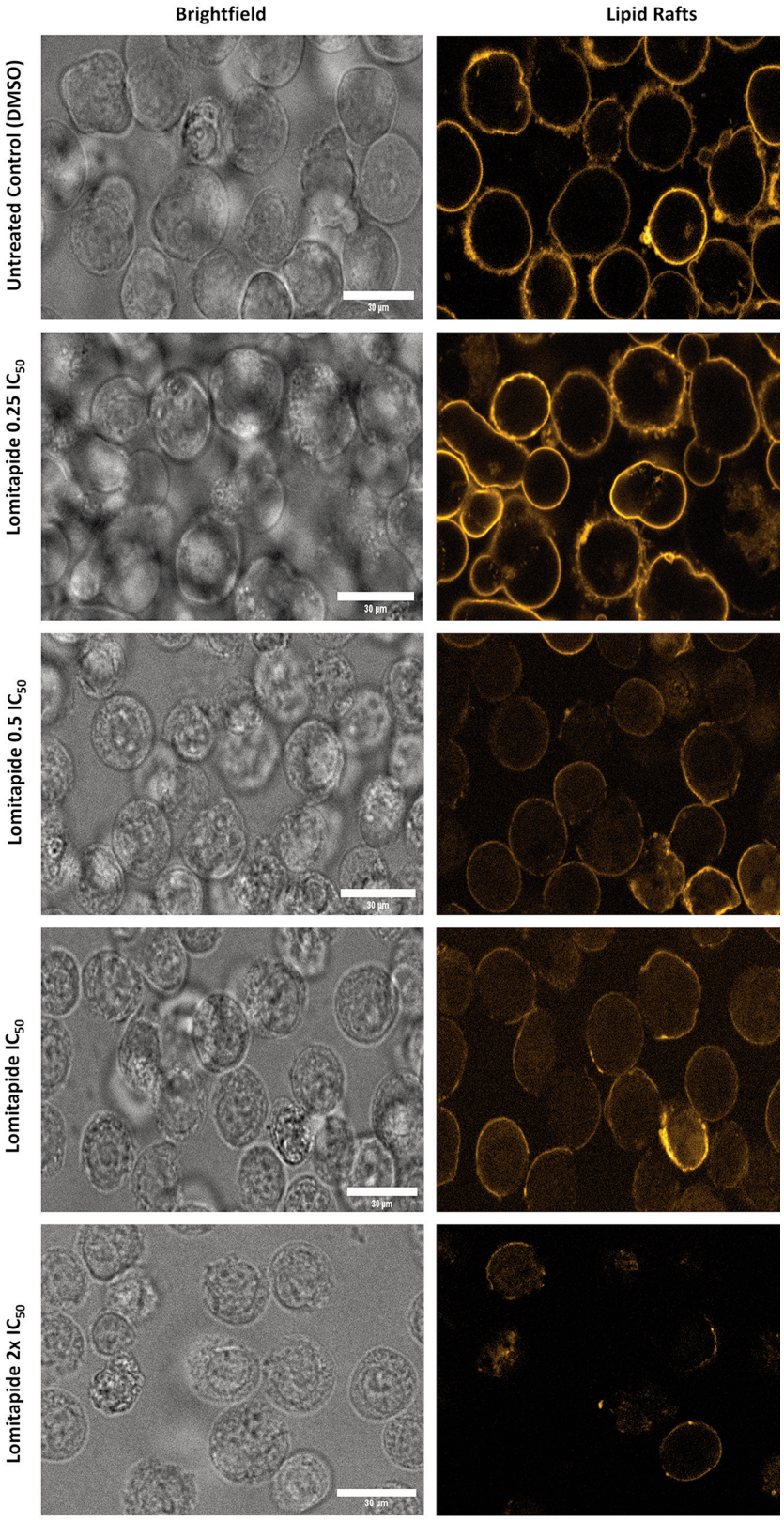

Figure 4. *Detection of lipid raft microdomain arrangements in NCI-H929 cells treated with varying concentrations of lomitapide (0.25×IC_{50}, 0.5×IC_{50}, IC_{50}, and 2×IC_{50}) by confocal microscopy.*

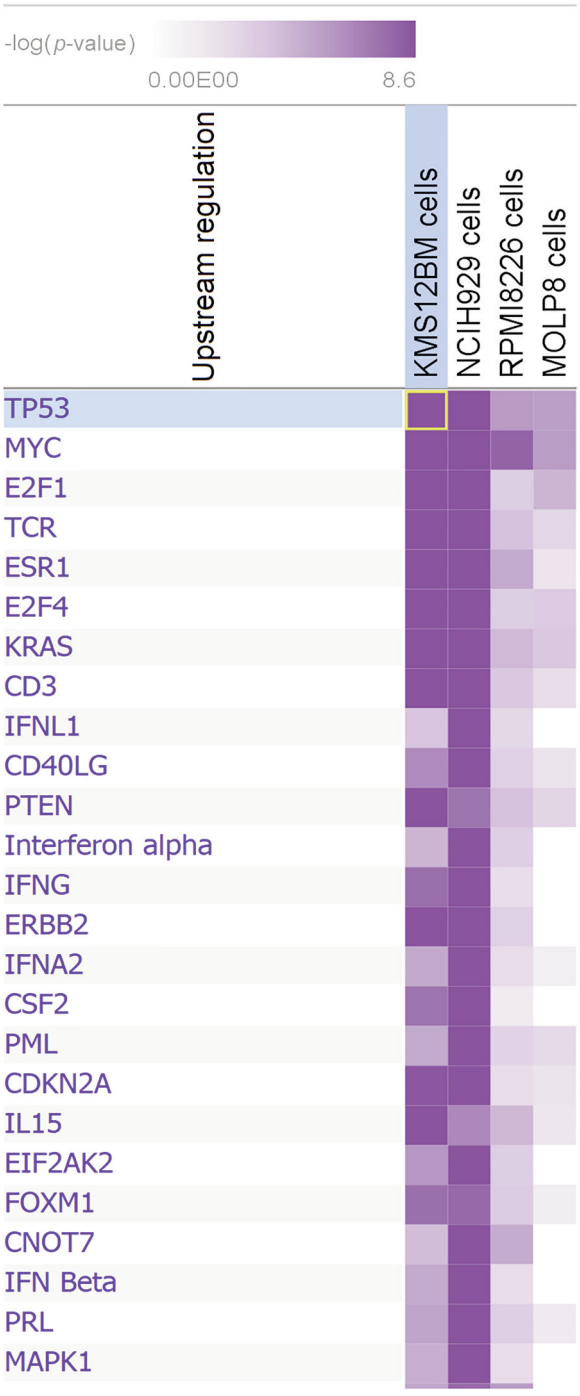

Figure 5. *Upstream regulator analysis of upstream transcription regulators affected by lomitapide as determined by the IPA program. TP53 and c-MYC were identified as top common upstream regulators in four lomitapide-treated MM cell lines (KMS-12-BM, NCI-H929, RPMI-8226 and MOLP-8) compared to their untreated counterparts.*

To further corroborate our finding that lomitapide triggers apoptosis in MM cells, PARP-1 expression was determined. PARP-1 is a nuclear protein that has a wide range of functions as an enzyme in the repair mechanism of the DNA such as base excision repair, nucleotide excision repair and single strand base repair. During apoptosis, PARP-1 is enzymatically cleaved by the activation of caspases, a family of cysteine proteases (51).

The IgGκ monoclonal antibody daratumumab is an immunomodulatory drug that targets CD38 and improved the outcomes of MM patients (52). Daratumumab kills MM cells by diverse mechanisms of action, including induction of apoptosis, complement-dependent cytotoxicity, antibody-dependent cell-mediated cytotoxicity, and antibody-dependent cellular phagocytosis (53), signal transduction (54), cell adhesion, and differentiation (55). Importantly, recent evidence suggested that CD38 enhanced proliferation and inhibited apoptosis of CD38-overexpressing cervical cancer cells by upregulation of MDM2, cyclin A1, CDK4, cyclin D1, NF-κB p65, and c-REL as well as downregulation of p53, p21, and p38 (56). Therefore, silencing CD38 is an attractive strategy to combat MM. This fits with our finding that downregulation of CD38 in response to lomitapide treatment triggered apoptosis in MM cells. Noteworthy, the CD38's regulator, BTK, plays a decisive role in the development, differentiation, and proliferation of B-lineage cells, making it an attractive target for the treatment of B-cell malignancies (57). Intriguingly, BTK was down-regulated upon lomitapide treatment.

Interestingly, gene expression profiling revealed that lomitapide leads to the de-regulation of genes that are potential activators or repressors of TP53 and c-MYC. Riley *et al*. compiled a list of p53-regulated genes and analyzed their p53 response elements in DNA that bind the p53 protein and promote transcriptional control (58). Intriguingly, our gene expression profile showed four up-regulated genes (*ATF3, CAV1, DUSP1* and *TNFRSF10B*) that can be transcriptionally activated by p53. Furthermore, several target genes for oncogenic c-MYC have been identified, and they might represent valuable therapeutic targets for inhibition tumor formation (59).

In our microarray analysis, 8 c-MYC target genes (*SRM, NOP56, PHB, HNRNPD, HSPD, PFKM, NME1,* and *LDHA*) were down-regulated in MM cells treated with lomitapide, indicating that lomitapide affects c-MYC downstream signaling. Notably, the cross-talk between p53 and c-MYC has been associated with the prognosis and progression of several hematologic malignancies (60).

C-MYC plays a critical role in evolving MGUS to MM, and its overexpression is a common trait for MM patients (61, 62). Cell cycle progression was associated with overexpression of c-MYC, whereas its downregulation induced cell cycle arrest and impaired mitogenic response (63). Wang *et al*. investigated 23 cell lines with short-hairpin-mediated depletion of *c-MYC* and noted that the

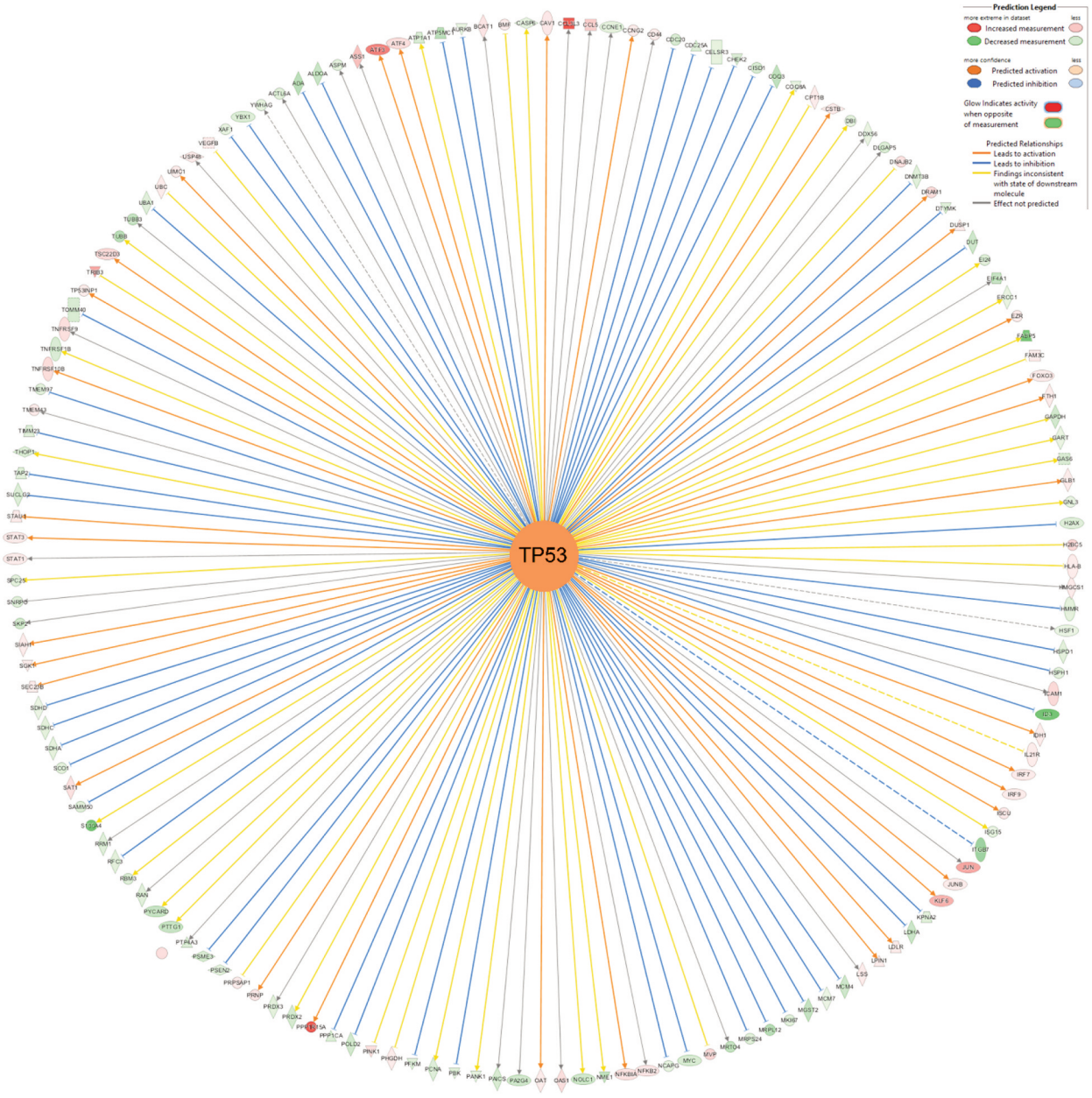

Figure 6. *Network of deregulated genes that were differentially expressed upon TP53 activation after lomitapide treatment as determined by Ingenuity Pathway Analysis. Color code: green, downregulation; red, upregulation.*

arrest took place at the G_0/G_1 phase in normal cells and some tumor-derived cell lines, whereas in other tumor cell lines the arrest occurred at G_2/M (64). Indeed, our results showed that lomitapide down-regulated *c-MYC* expression in treated MM cells, and as a consequence arrested the cell cycle in the G_0/G_1 phase, and cellular population accumulated in sub-G_0/G_1. Furthermore, c-MYC was also associated with apoptotic response. In 32Dcl3 myeloid progenitor cells, withdrawal of IL-3 resulted in c-MYC downregulation, cellular accumulation in the G_0/G_1 phase of the cell cycle, and rapid induction of apoptosis (65). The results in these myeloid progenitor cells are in accordance with our results in MM cells.

The guardian of the genome, p53, is a nuclear phosphoprotein that acts biochemically as a transcription factor and biologically as a powerful tumor suppressor (66). Under cellular stress conditions such as genotoxic damages, oncogene activation, and hypoxia, p53 responds by induction

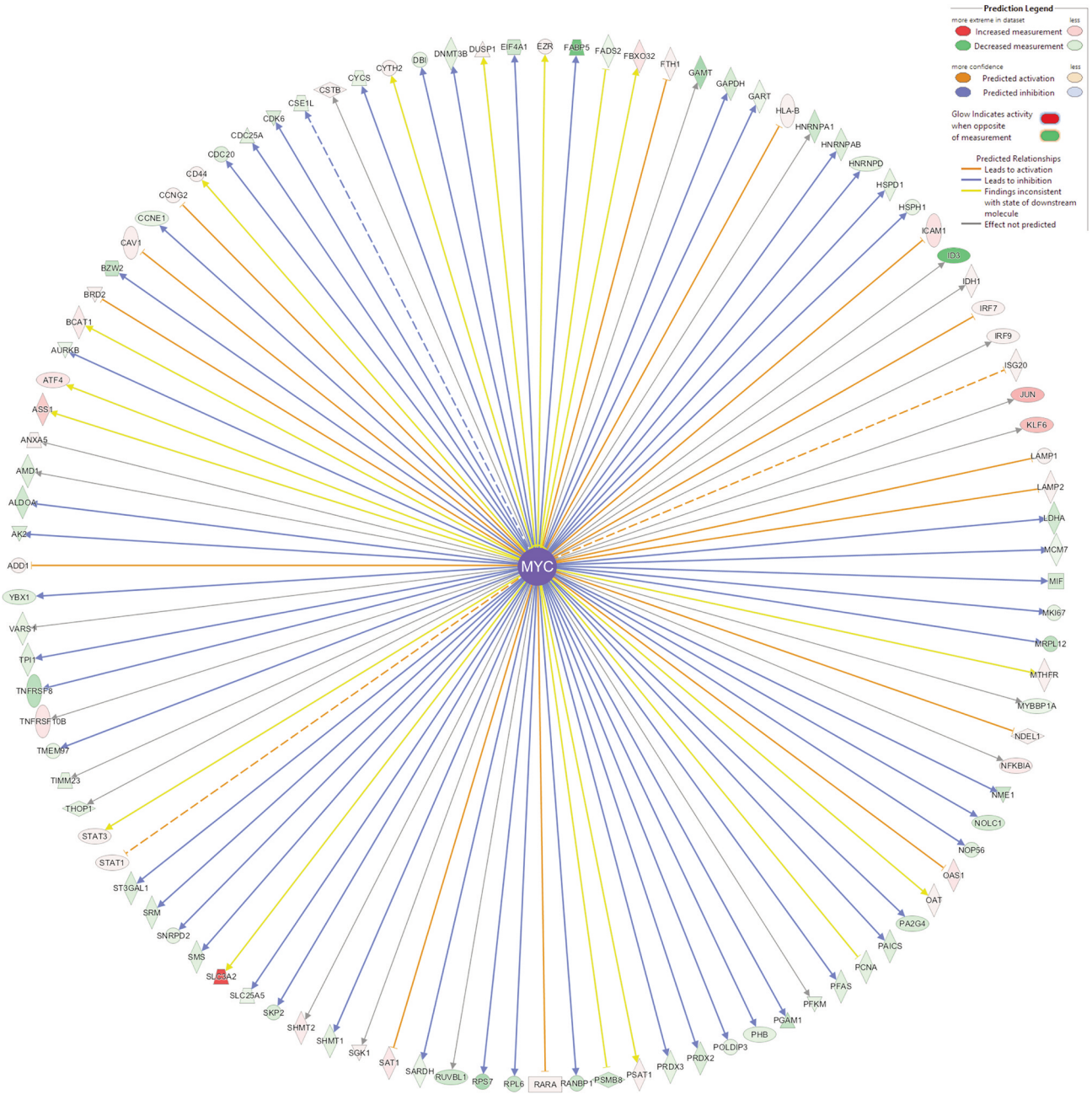

Figure 7. *Network of deregulated genes that were differentially expressed upon c-MYC inhibition after lomitapide treatment as determined by Ingenuity Pathway Analysis. Color code: green, downregulation; red, upregulation.*

of cell cycle arrest and/or apoptosis (67). The alternate reading frame (ARF) is a master regulator for the cross-talk between p53 and c-MYC (68). ARF inhibited the p53 negative regulator, MDM2, function and at the same time negatively regulated the transcriptional activity of c-MYC (69). Both effects result in p53 overexpression and activation, thus facilitating p53-dependent cell cycle arrest and apoptosis. Additionally, p53 enhances apoptosis through transcriptional activation of the FAS/CD95 death receptor. The activated FAS death domain forms a cytoplasmic docking site for the adapter protein FADD, which recruits procaspase-8 to promote its autocatalytic activation, thereby initiating the apoptotic cascade (70, 71). Of note, lipid rafts constitute a linchpin that drives FAS/CD95 death signaling

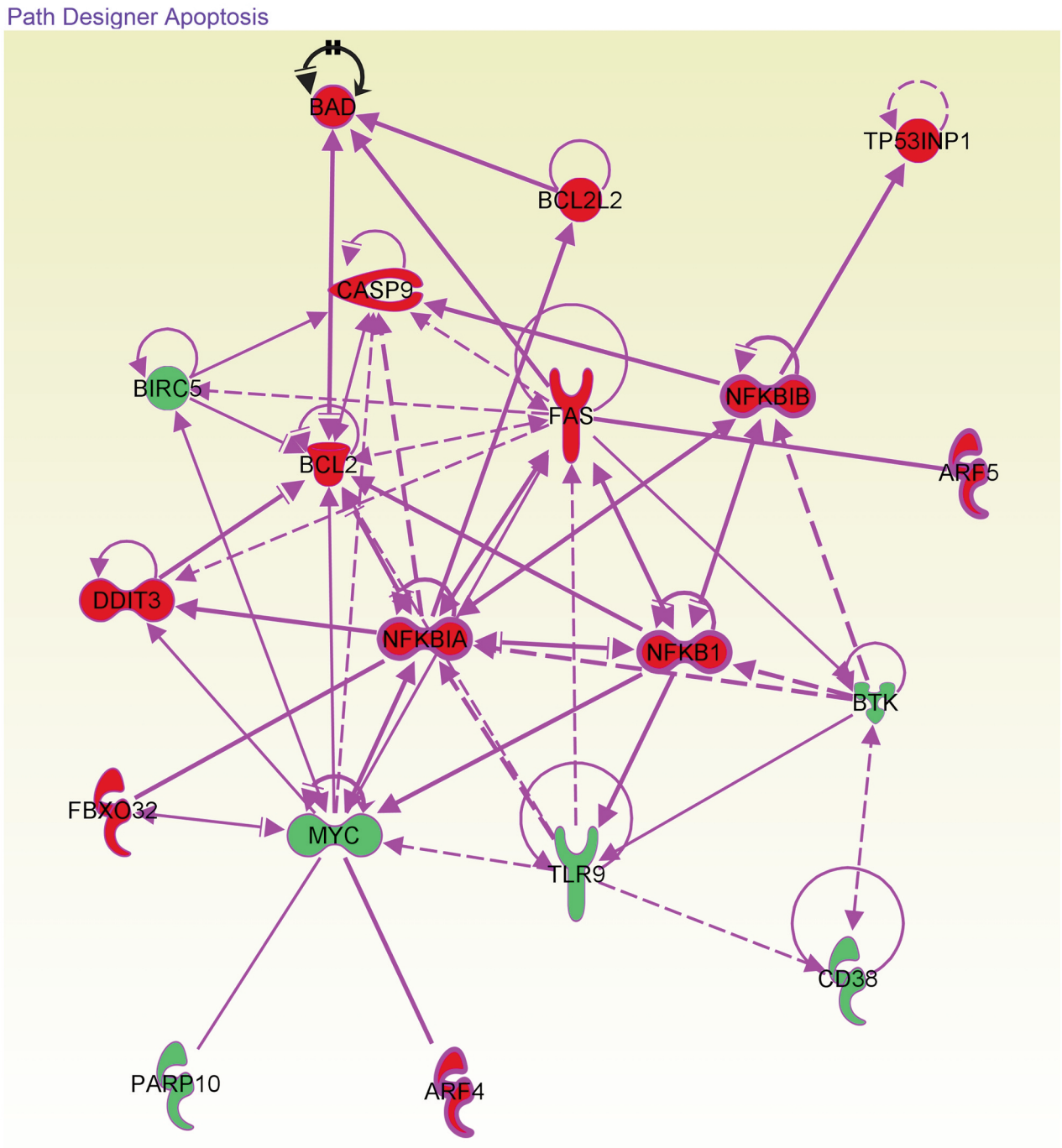

Figure 8. *Network of deregulated genes that were differentially expressed upon c-MYC inhibition after lomitapide treatment as determined by Ingenuity Pathway Analysis. Color code: green, downregulation; red, upregulation.*

(39, 72). Remarkably, our gene expression profiling results revealed overexpression of *FAS* and *ARF* upon treatment of MM cells with lomitapide. In conclusion, we found that the induction of apoptosis *via* a lipid raft-associated CD38-BTK-p53-c-MYC axis may represent an important mechanism of action of lomitapide towards MM cells. This drug that was initially launched to treat homozygous familiar hypercholesterolemia may, therefore, be reconsidered for treatment of MM, which is still an incurable disease with short survival rates.

Funding

We are grateful to a donation of Mr. Marc Stobel, Frankfurt a.M., Germany. The study was intramurally funded. E.L. is supported by the Deutsche Krebshilfe (process number: 70112693).

Conflicts of Interest

The Authors declare that there are no conflicts of interest.

Authors' Contributions

M.E.M.S. performed bioinformatics, flow cytometry, and confocal microscopy, and wrote the draft of the manuscript. J.C.B and S.B.M. performed western blotting. E.L. and M.C. provided the cell lines and edited the manuscript. T.E. supervised the project and wrote and edited the paper.

Acknowledgements

We thank the Microarray Unit of the Genomics and Proteomics Core Facility, German Cancer Research Center (DKFZ, Heidelberg), for providing excellent Expression Profiling services.

References

1 van de Donk NWCJ, Pawlyn C and Yong KL: Multiple myeloma. Lancet *397(10272)*: 410-427, 2021. PMID: 33516340. DOI: 10.1016/S0140-6736(21)00135-5

2 Kuehl WM and Bergsagel PL: Multiple myeloma: evolving genetic events and host interactions. Nat Rev Cancer *2(3)*: 175-187, 2002. PMID: 11990854. DOI: 10.1038/nrc746

3 Rajkumar SV, Dimopoulos MA, Palumbo A, Blade J, Merlini G, Mateos MV, Kumar S, Hillengass J, Kastritis E, Richardson P, Landgren O, Paiva B, Dispenzieri A, Weiss B, LeLeu X, Zweegman S, Lonial S, Rosinol L, Zamagni E, Jagannath S, Sezer O, Kristinsson SY, Caers J, Usmani SZ, Lahuerta JJ, Johnsen HE, Beksac M, Cavo M, Goldschmidt H, Terpos E, Kyle RA, Anderson KC, Durie BG and Miguel JF: International Myeloma Working Group updated criteria for the diagnosis of multiple myeloma. Lancet Oncol *15(12)*: e538-e548, 2014. PMID: 25439696. DOI: 10.1016/S1470-2045(14)70442-5

4 Röllig C, Knop S and Bornhäuser M: Multiple myeloma. Lancet *385(9983)*: 2197-2208, 2015. PMID: 25540889. DOI: 10.1016/S0140-6736(14)60493-1

5 Kumar SK, Rajkumar V, Kyle RA, van Duin M, Sonneveld P, Mateos MV, Gay F and Anderson KC: Multiple myeloma. Nat Rev Dis Primers *3*: 17046, 2017. PMID: 28726797. DOI: 10.1038/nrdp.2017.46

6 Landgren O, Gridley G, Turesson I, Caporaso NE, Goldin LR, Baris D, Fears TR, Hoover RN and Linet MS: Risk of monoclonal gammopathy of undetermined significance (MGUS) and subsequent multiple myeloma among African American and white veterans in the United States. Blood *107(3)*: 904-906, 2006. PMID: 16210333. DOI: 10.1182/blood-2005-08-3449

7 Michel V and Bakovic M: Lipid rafts in health and disease. Biol Cell *99(3)*: 129-140, 2007. PMID: 17064251. DOI: 10.1042/BC20060051

8 Mañes S, del Real G and Martínez-A C: Pathogens: raft hijackers. Nat Rev Immunol *3(7)*: 557-568, 2003. PMID: 12876558. DOI: 10.1038/nri1129

9 Pavón EJ, Muñoz P, Navarro MD, Raya-Alvarez E, Callejas-Rubio JL, Navarro-Pelayo F, Ortego-Centeno N, Sancho J and Zubiaur M: Increased association of CD38 with lipid rafts in T cells from patients with systemic lupus erythematosus and in activated normal T cells. Mol Immunol *43(7)*: 1029-1039, 2006. PMID: 15964076. DOI: 10.1016/j.molimm.2005.05.002

10 van de Donk NWCJ, Richardson PG and Malavasi F: CD38 antibodies in multiple myeloma: back to the future. Blood *131(1)*: 13-29, 2018. PMID: 29118010. DOI: 10.1182/blood-2017-06-740944

11 Lee HC: Enzymatic functions and structures of CD38 and homologs. Chem Immunol *75*: 39-59, 2000. PMID: 10851778. DOI: 10.1159/000058774

12 Lande R, Urbani F, Di Carlo B, Sconocchia G, Deaglio S, Funaro A, Malavasi F and Ausiello CM: CD38 ligation plays a direct role in the induction of IL-1beta, IL-6, and IL-10 secretion in resting human monocytes. Cell Immunol *220(1)*: 30-38, 2002. PMID: 12718937. DOI: 10.1016/s0008-8749(03)00025-x

13 Mallone R, Funaro A, Zubiaur M, Baj G, Ausiello CM, Tacchetti C, Sancho J, Grossi C and Malavasi F: Signaling through CD38 induces NK cell activation. Int Immunol *13(4)*: 397-409, 2001. PMID: 11282979. DOI: 10.1093/intimm/13.4.397

14 Funaro A, Morra M, Calosso L, Zini MG, Ausiello CM and Malavasi F: Role of the human CD38 molecule in B cell activation and proliferation. Tissue Antigens *49(1)*: 7-15, 1997. PMID: 9027959. DOI: 10.1111/j.1399-0039.1997.tb02703.x

15 Ausiello CM, la Sala A, Ramoni C, Urbani F, Funaro A and Malavasi F: Secretion of IFN-gamma, IL-6, granulocyte-macrophage colony-stimulating factor and IL-10 cytokines after activation of human purified T lymphocytes upon CD38 ligation. Cell Immunol *173(2)*: 192-197, 1996. PMID: 8912876. DOI: 10.1006/cimm.1996.0267

16 Fedele G, Frasca L, Palazzo R, Ferrero E, Malavasi F and Ausiello CM: CD38 is expressed on human mature monocyte-derived dendritic cells and is functionally involved in CD83 expression and IL-12 induction. Eur J Immunol *34(5)*: 1342-1350, 2004. PMID: 15114667. DOI: 10.1002/eji.200324728

17 Trubiani O, Guarnieri S, Orciani M, Salvolini E and Di Primio R: Sphingolipid microdomains mediate CD38 internalization: topography of the endocytosis. Int J Immunopathol Pharmacol *17(3)*: 293-300, 2004. PMID: 15461863. DOI: 10.1177/039463200401700309

18 Rawlings DJ, Saffran DC, Tsukada S, Largaespada DA, Grimaldi JC, Cohen L, Mohr RN, Bazan JF, Howard M and Copeland NG: Mutation of unique region of Bruton's tyrosine kinase in immunodeficient XID mice. Science *261(5119)*: 358-361, 1993. PMID: 8332901. DOI: 10.1126/science.8332901

19 Santos-Argumedo L, Lund FE, Heath AW, Solvason N, Wu WW, Grimaldi JC, Parkhouse RM and Howard M: CD38 unresponsiveness of xid B cells implicates Bruton's tyrosine kinase (btk) as a regular of CD38 induced signal transduction. Int Immunol *7(2)*: 163-170, 1995. PMID: 7734414. DOI: 10.1093/intimm/7.2.163

20 Liu Y, Dong Y, Jiang QL, Zhang B and Hu AM: Bruton's tyrosine kinase: potential target in human multiple myeloma. Leuk Lymphoma *55(1)*: 177-181, 2014. PMID: 23581641. DOI: 10.3109/10428194.2013.794458

21 de Gorter DJ, Beuling EA, Kersseboom R, Middendorp S, van Gils JM, Hendriks RW, Pals ST and Spaargaren M: Bruton's tyrosine kinase and phospholipase Cgamma2 mediate chemokine-controlled B cell migration and homing. Immunity *26(1)*: 93-104, 2007. PMID: 17239630. DOI: 10.1016/j.immuni.2006.11.012

22 Cuchel M, Bruckert E, Ginsberg HN, Raal FJ, Santos RD, Hegele RA, Kuivenhoven JA, Nordestgaard BG, Descamps OS, Steinhagen-Thiessen E, Tybjærg-Hansen A, Watts GF, Averna M, Boileau C, Borén J, Catapano AL, Defesche JC, Hovingh GK, Humphries SE, Kovanen PT, Masana L, Pajukanta P, Parhofer KG, Ray KK, Stalenhoef AF, Stroes E, Taskinen MR, Wiegman A, Wiklund O, Chapman MJ and European Atherosclerosis Society Consensus Panel on Familial Hypercholesterolaemia: Homozygous familial hypercholesterolaemia: new insights and guidance for clinicians to improve detection and clinical management. A position paper from the Consensus Panel on Familial Hypercholesterolaemia of the European Atherosclerosis Society. Eur Heart J *35(32)*: 2146-2157, 2014. PMID: 25053660. DOI: 10.1093/eurheartj/ehu274

23 Alonso R, Cuevas A and Mata P: Lomitapide: a review of its clinical use, efficacy, and tolerability. Core Evid *14*: 19-30, 2019. PMID: 31308834. DOI: 10.2147/CE.S174169

24 Rader DJ and Kastelein JJ: Lomitapide and mipomersen: two first-in-class drugs for reducing low-density lipoprotein cholesterol in patients with homozygous familial hypercholesterolemia. Circulation *129(9)*: 1022-1032, 2014. PMID: 24589695. DOI: 10.1161/CIRCULATIONAHA.113.001292

25 Ashburn TT and Thor KB: Drug repositioning: identifying and developing new uses for existing drugs. Nat Rev Drug Discov *3(8)*: 673-683, 2004. PMID: 15286734. DOI: 10.1038/nrd1468

26 Vargesson N: Thalidomide-induced teratogenesis: history and mechanisms. Birth Defects Res C Embryo Today *105(2)*: 140-156, 2015. PMID: 26043938. DOI: 10.1002/bdrc.21096

27 Efferth T: Beyond malaria: The inhibition of viruses by artemisinin-type compounds. Biotechnol Adv *36(6)*: 1730-1737, 2018. PMID: 29305894. DOI: 10.1016/j.biotechadv.2018.01.001

28 Efferth T, Dunstan H, Sauerbrey A, Miyachi H and Chitambar CR: The anti-malarial artesunate is also active against cancer. Int J Oncol *18(4)*: 767-773, 2001. PMID: 11251172. DOI: 10.3892/ijo.18.4.767

29 Krishna S, Ganapathi S, Ster IC, Saeed ME, Cowan M, Finlayson C, Kovacsevics H, Jansen H, Kremsner PG, Efferth T and Kumar D: A randomised, double blind, placebo-controlled pilot study of oral artesunate therapy for colorectal cancer. EBioMedicine *2(1)*: 82-90, 2014. PMID: 26137537. DOI: 10.1016/j.ebiom.2014.11.010

30 Jansen FH, Adoubi I, J C KC, DE Cnodder T, Jansen N, Tschulakow A and Efferth T: First study of oral Artenimol-R in advanced cervical cancer: clinical benefit, tolerability and tumor markers. Anticancer Res *31(12)*: 4417-4422, 2011. PMID: 22199309.

31 Saeed MEM, Breuer E, Hegazy MF and Efferth T: Retrospective study of small pet tumors treated with Artemisia annua and iron. Int J Oncol *56(1)*: 123-138, 2020. PMID: 31789393. DOI: 10.3892/ijo.2019.4921

32 Protein Data Bank. Available at: http://www.rcsb.org/pdb [Last accessed on January 31, 2022]

33 DrugBank FDA only. Available at: https://zinc.docking.org/catalogs/dbfda/ [Last accessed on June 6, 2022]

34 Morris G, Goodsell D, Halliday R, Huey R, Hart W, Belew R and Olson A: Automated docking using a Lamarckian genetic algorithm and an empirical binding free energy function. J Computat Chem *19(14)*: 1639-1662, 2021. DOI: 10.1002/(SICI)1096-987X(19981115)19:14<1639::AID-JCC10>3.0.CO;2-B

35 O'Brien J, Wilson I, Orton T and Pognan F: Investigation of the Alamar Blue (resazurin) fluorescent dye for the assessment of mammalian cell cytotoxicity. Eur J Biochem *267(17)*: 5421-5426, 2000. PMID: 10951200. DOI: 10.1046/j.1432-1327.2000.01606.x

36 Adham AN, Abdelfatah S, Naqishbandi AM, Mahmoud N and Efferth T: Cytotoxicity of apigenin toward multiple myeloma cell lines and suppression of iNOS and COX-2 expression in STAT1-transfected HEK293 cells. Phytomedicine *80*: 153371, 2021. PMID: 33070080. DOI: 10.1016/j.phymed.2020.153371

37 Hegazy MF, Dawood M, Mahmoud N, Elbadawi M, Sugimoto Y, Klauck SM, Mohamed N and Efferth T: 2α-Hydroxyalantolactone from *Pulicaria undulata*: activity against multidrug-resistant tumor cells and modes of action. Phytomedicine *81*: 153409, 2021. PMID: 33341310. DOI: 10.1016/j.phymed.2020.153409

38 Eberwine J, Yeh H, Miyashiro K, Cao Y, Nair S, Finnell R, Zettel M and Coleman P: Analysis of gene expression in single live neurons. Proc Natl Acad Sci USA *89(7)*: 3010-3014, 1992. PMID: 1557406. DOI: 10.1073/pnas.89.7.3010

39 Gajate C, Del Canto-Jañez E, Acuña AU, Amat-Guerri F, Geijo E, Santos-Beneit AM, Veldman RJ and Mollinedo F: Intracellular triggering of Fas aggregation and recruitment of apoptotic molecules into Fas-enriched rafts in selective tumor cell apoptosis. J Exp Med *200(3)*: 353-365, 2004. PMID: 15289504. DOI: 10.1084/jem.20040213

40 Alves ACS, Dias RA, Kagami LP, das Neves GM, Torres FC, Eifler-Lima VL, Carvalho I, de Miranda Silva C and Kawano DF: Beyond the "Lock and Key" paradigm: Targeting lipid rafts to induce the selective apoptosis of cancer cells. Curr Med Chem *25(18)*: 2082-2104, 2018. PMID: 29332565. DOI: 10.2174/0929867325666180111100601

41 Shaughnessy AF: Old drugs, new tricks. BMJ *342*: d741, 2011. PMID: 21307112. DOI: 10.1136/bmj.d741

42 Hughes JP, Rees S, Kalindjian SB and Philpott KL: Principles of early drug discovery. Br J Pharmacol *162(6)*: 1239-1249, 2011. PMID: 21091654. DOI: 10.1111/j.1476-5381.2010.01127.x

43 Radišauskas R, Kuzmickienė I, Milinavičienė E and Everatt R: Hypertension, serum lipids and cancer risk: A review of epidemiological evidence. Medicina (Kaunas) *52(2)*: 89-98, 2016. PMID: 27170481. DOI: 10.1016/j.medici.2016.03.002

44 Simons K and Toomre D: Lipid rafts and signal transduction. Nat Rev Mol Cell Biol *1(1)*: 31-39, 2000. PMID: 11413487. DOI: 10.1038/35036052

45 Jones RJ, Gu D, Bjorklund CC, Kuiatse I, Remaley AT, Bashir T, Vreys V and Orlowski RZ: The novel anticancer agent JNJ-26854165 induces cell death through inhibition of cholesterol transport and degradation of ABCA1. J Pharmacol Exp Ther *346(3)*: 381-392, 2013. PMID: 23820125. DOI: 10.1124/jpet.113.204958

46 Hungria VT, Latrilha MC, Rodrigues DG, Bydlowski SP, Chiattone CS and Maranhão RC: Metabolism of a cholesterol-rich microemulsion (LDE) in patients with multiple myeloma and a preliminary clinical study of LDE as a drug vehicle for the

treatment of the disease. Cancer Chemother Pharmacol *53(1)*: 51-60, 2004. PMID: 14574458. DOI: 10.1007/s00280-003-0692-y
47 Katz MS: Therapy insight: Potential of statins for cancer chemoprevention and therapy. Nat Clin Pract Oncol *2(2)*: 82-89, 2005. PMID: 16264880. DOI: 10.1038/ncponc0097
48 Chan KK, Oza AM and Siu LL: The statins as anticancer agents. Clin Cancer Res *9(1)*: 10-19, 2003. PMID: 12538446.
49 Murai T: The role of lipid rafts in cancer cell adhesion and migration. Int J Cell Biol *2012*: 763283, 2012. PMID: 22253629. DOI: 10.1155/2012/763283
50 Jeon JH, Kim SK, Kim HJ, Chang J, Ahn CM and Chang YS: Lipid raft modulation inhibits NSCLC cell migration through delocalization of the focal adhesion complex. Lung Cancer *69(2)*: 165-171, 2010. PMID: 19945766. DOI: 10.1016/j.lungcan.2009.10.014
51 Chaitanya GV, Steven AJ and Babu PP: PARP-1 cleavage fragments: signatures of cell-death proteases in neurodegeneration. Cell Commun Signal *8*: 31, 2010. PMID: 21176168. DOI: 10.1186/1478-811X-8-31
52 Krejcik J, Casneuf T, Nijhof IS, Verbist B, Bald J, Plesner T, Syed K, Liu K, van de Donk NW, Weiss BM, Ahmadi T, Lokhorst HM, Mutis T and Sasser AK: Daratumumab depletes CD38+ immune regulatory cells, promotes T-cell expansion, and skews T-cell repertoire in multiple myeloma. Blood *128(3)*: 384-394, 2016. PMID: 27222480. DOI: 10.1182/blood-2015-12-687749
53 Palumbo A, Chanan-Khan A, Weisel K, Nooka AK, Masszi T, Beksac M, Spicka I, Hungria V, Munder M, Mateos MV, Mark TM, Qi M, Schecter J, Amin H, Qin X, Deraedt W, Ahmadi T, Spencer A, Sonneveld P and CASTOR Investigators: Daratumumab, Bortezomib, and Dexamethasone for multiple myeloma. N Engl J Med *375(8)*: 754-766, 2016. PMID: 27557302. DOI: 10.1056/NEJMoa1606038
54 Rah SY and Kim UH: CD38-mediated Ca(2+) signaling contributes to glucagon-induced hepatic gluconeogenesis. Sci Rep *5*: 10741, 2015. PMID: 26038839. DOI: 10.1038/srep10741
55 Malavasi F, Funaro A, Roggero S, Horenstein A, Calosso L and Mehta K: Human CD38: a glycoprotein in search of a function. Immunol Today *15(3)*: 95-97, 1994. PMID: 8172650. DOI: 10.1016/0167-5699(94)90148-1
56 Liao S, Xiao S, Chen H, Zhang M, Chen Z, Long Y, Gao L, Zhu G, He J, Peng S, Xiong W, Zeng Z, Li Z, Zhou M, Li X, Ma J, Wu M, Xiang J, Li G and Zhou Y: CD38 enhances the proliferation and inhibits the apoptosis of cervical cancer cells by affecting the mitochondria functions. Mol Carcinog *56(10)*: 2245-2257, 2017. PMID: 28544069. DOI: 10.1002/mc.22677
57 Robak T and Robak E: Tyrosine kinase inhibitors as potential drugs for B-cell lymphoid malignancies and autoimmune disorders. Expert Opin Investig Drugs *21(7)*: 921-947, 2012. PMID: 22612424. DOI: 10.1517/13543784.2012.685650
58 Riley T, Sontag E, Chen P and Levine A: Transcriptional control of human p53-regulated genes. Nat Rev Mol Cell Biol *9(5)*: 402-412, 2008. PMID: 18431400. DOI: 10.1038/nrm2395
59 Menssen A and Hermeking H: Characterization of the c-MYC-regulated transcriptome by SAGE: identification and analysis of c-MYC target genes. Proc Natl Acad Sci USA *99(9)*: 6274-6279, 2002. PMID: 11983916. DOI: 10.1073/pnas.082005599
60 Yu L, Yu TT and Young KH: Cross-talk between Myc and p53 in B-cell lymphomas. Chronic Dis Transl Med *5(3)*: 139-154, 2019. PMID: 31891126. DOI: 10.1016/j.cdtm.2019.08.001
61 Szabo AG, Gang AO, Pedersen MØ, Poulsen TS, Klausen TW and Nørgaard P: Overexpression of c-myc is associated with adverse clinical features and worse overall survival in multiple myeloma. Leuk Lymphoma *57(11)*: 2526-2534, 2016. PMID: 27243588. DOI: 10.1080/10428194.2016.1187275
62 Kuehl WM and Bergsagel PL: MYC addiction: a potential therapeutic target in MM. Blood *120(12)*: 2351-2352, 2012. PMID: 22996653. DOI: 10.1182/blood-2012-08-445262
63 Bretones G, Delgado MD and León J: Myc and cell cycle control. Biochim Biophys Acta *1849(5)*: 506-516, 2015. PMID: 24704206. DOI: 10.1016/j.bbagrm.2014.03.013
64 Wang H, Mannava S, Grachtchouk V, Zhuang D, Soengas MS, Gudkov AV, Prochownik EV and Nikiforov MA: c-Myc depletion inhibits proliferation of human tumor cells at various stages of the cell cycle. Oncogene *27(13)*: 1905-1915, 2008. PMID: 17906696. DOI: 10.1038/sj.onc.1210823
65 Askew DS, Ashmun RA, Simmons BC and Cleveland JL: Constitutive c-myc expression in an IL-3-dependent myeloid cell line suppresses cell cycle arrest and accelerates apoptosis. Oncogene *6(10)*: 1915-1922, 1991. PMID: 1923514.
66 Wang Z and Sun Y: Targeting p53 for novel anticancer therapy. Transl Oncol *3(1)*: 1-12, 2010. PMID: 20165689. DOI: 10.1593/tlo.09250
67 Vogelstein B, Lane D and Levine AJ: Surfing the p53 network. Nature *408(6810)*: 307-310, 2000. PMID: 11099028. DOI: 10.1038/35042675
68 Hoffman B and Liebermann DA: Apoptotic signaling by c-MYC. Oncogene *27(50)*: 6462-6472, 2008. PMID: 18955973. DOI: 10.1038/onc.2008.312
69 Sarkar D and Fisher PB: Regulation of Myc function by ARF: checkpoint for Myc-induced oncogenesis. Cancer Biol Ther *5(6)*: 693-695, 2006. PMID: 16775430. DOI: 10.4161/cbt.5.6.2939
70 Muzio M, Stockwell BR, Stennicke HR, Salvesen GS and Dixit VM: An induced proximity model for caspase-8 activation. J Biol Chem *273(5)*: 2926-2930, 1998. PMID: 9446604. DOI: 10.1074/jbc.273.5.2926
71 Huang DC, Hahne M, Schroeter M, Frei K, Fontana A, Villunger A, Newton K, Tschopp J and Strasser A: Activation of Fas by FasL induces apoptosis by a mechanism that cannot be blocked by Bcl-2 or Bcl-x(L). Proc Natl Acad Sci USA *96(26)*: 14871-14876, 1999. PMID: 10611305. DOI: 10.1073/pnas.96.26.14871
72 Gajate C, Fonteriz RI, Cabaner C, Alvarez-Noves G, Alvarez-Rodriguez Y, Modolell M and Mollinedo F: Intracellular triggering of Fas, independently of FasL, as a new mechanism of antitumor ether lipid-induced apoptosis. Int J Cancer *85(5)*: 674-682, 2000. PMID: 10699948. DOI: 10.1002/(sici)1097-0215(20000301)85:5<674::aid-ijc13>3.0.co;2-z

Received April 13, 2022
Revised May 9, 2022
Accepted June 6, 2022